

## – Supplemental Material –

### DERIVATION OF $\alpha_-$ EXTRACTION METHOD

The determination of  $\alpha_-$  and the correction factors  $c, l$  raises statistical challenges. Additional details for the statistical analysis in the main text are provided here. To clarify the notation, random variables (RVs) are denoted with calligraphic symbols ( $\mathcal{F}, \mathcal{O}, \mathcal{C}$ ) while the values they can take are denoted with ordinary letters; in particular, we use  $O$  for observables with reported  $\mu, \sigma$ , and  $f$  for Fierz values.

Consider the measurement of observables  $\mathcal{C}_{j,i}; j = 1, \dots, 7$  for  $n$  kinematic points  $(W_i, \cos \theta_i)$ , i.e.,  $i = 1, \dots, n$ . We assume that all measurements of  $\mathcal{C}$  are independent and normally distributed,  $\mathcal{C}_{j,i} \sim \mathcal{N}[\mu_{\mathcal{C}_{j,i}}, \sigma_{\mathcal{C}_{j,i}}^2]$ . These “raw” data correspond to the actual measurements, for example the product  $\alpha_- P$  in Eq. (1) of the main text. In the subsequent experimental analysis of the CLAS data, the  $\mathcal{C}_{j,i}$  are all scaled by the (now questioned) pre-2019 PDG value for the weak decay parameter  $\tilde{\alpha}_- \equiv \alpha_-^{\text{old}} = 0.642$  to obtain  $\mathcal{O}_{j,i} \sim \mathcal{N}[\mu_{j,i} \equiv \mu_{\mathcal{C}_{j,i}}/\tilde{\alpha}_-, \sigma_{j,i}^2 \equiv \sigma_{\mathcal{C}_{j,i}}^2/\tilde{\alpha}_-^2]$  which correspond to the published data and which are the quantities entering the Fierz identities.

We determine corrections to  $\tilde{\alpha}_-$  by introducing a calibration factor  $a = \tilde{\alpha}_-/\alpha_-$  to scale the observables entering the Fierz identities,  $\mathcal{O}_{j,i} \rightarrow a\mathcal{O}_{j,i}$ . The parameters  $a, l, c$  are estimators, usually denoted as  $\hat{a}, \hat{l}, \hat{c}$ , but we leave out the hats in favor of a simplified notation. For the formal discussion in this supplemental material, we set the true, unknown  $\alpha_-$  to one for simplicity. Note that, while there are a finite number of  $n$  measurements, we have to consider the ensemble limit  $m \rightarrow \infty$  to check for biases, i.e., the expectation values of the parameter estimators  $a, l, c$  for a finite number of kinematic points. To derive the distributions of the calibration parameters  $a, l, c$  we follow the same numbering as in the main text:

**1.** and **2.** *Bias when data errors are scaled/a-dependence of normalization constant.*

These two issues can best be discussed together. Here, we consider the inverse of  $a$ ,  $b = 1/a$ <sup>1</sup>, meaning that we have to show for the expectation value  $E[b] = \tilde{\alpha}_-^{-1}$  for any method to be unbiased so that the true  $\alpha_- = \alpha_-^{\text{old}} b$  (all statements in the sense of pdfs, to be formalized below). To demonstrate the issue we start with the simplest Fierz identity,  $E[\mathcal{O}_i/b] = 1$ , i.e.,  $\mu \equiv E[\mu_{\mathcal{C}_i}] = 1$  (the index  $j$

TABLE I. Ordering of observables and pertinent combinations  $s_j$  of correction factors for the first Fierz identity.

$\mathcal{O}_{j,i}$	$\mathcal{O}_{x,i}$	$\mathcal{O}_{z,i}$	$\mathcal{T}_i$	$\mathcal{C}_{x,i}$	$\mathcal{C}_{z,i}$	$\Sigma_i$	$\mathcal{P}_i$
$s_j$	$a^2 l^2$	$a^2 l^2$	$-a^2 l^2$	$a^2 c^2$	$a^2 c^2$	$l^2$	$a^2$

is dropped here because there is only one observable  $j$ ). The Fierz values are given by  $\mathcal{F}_i = \mathcal{O}_i/b$  and distributed as  $(f_i = \mathcal{O}_i/b, b > 0)$ ,

$$p_{\mathcal{F}_i}^{(1)}(f_i, b) = \int d\mathcal{O}_i p(\mathcal{O}_i) \delta(\mathcal{O}_i/b - f_i) = b p(b f_i). \quad (1)$$

The distribution of  $b$  is the conditional probability from the expected Fierz value at  $f_i = 1$ ,

$$p_i^{(1)}(b) = \frac{b}{\sqrt{2\pi}\mu_i\sigma_i} \exp\left[-\frac{(1-\mu_i/b)^2}{2(\sigma_i/b)^2}\right] \sim p_{\mathcal{F}_i}^{(1)}(1, b), \quad (2)$$

with mode at

$$b_i^{(1)} = \frac{\mu_{\mathcal{C}_i} + \sqrt{\mu_{\mathcal{C}_i}^2 + 4\sigma_{\mathcal{C}_i}^2}}{2\tilde{\alpha}_-}, \quad (3)$$

which is equal to  $\tilde{\alpha}_-^{-1}$  if and only if  $\sigma_{\mathcal{C}_i} \rightarrow 0$ , i.e., the obtained result is biased (even without considering the expectation value).

Next, consider the case in which  $b$  is removed from the normalization but still present for the scaling of  $\sigma_i$  in the exponent,

$$p_i^{(2)}(b) = \frac{1}{\sqrt{2\pi}\sigma_i} \exp\left[-\frac{(1-\mu_i/b)^2}{2(\sigma_i/b)^2}\right], \quad (4)$$

with mode at  $b_i^{(2)} = \mu_{\mathcal{C}_i}/\tilde{\alpha}_-$  so that  $E[b_i^{(2)}] = \tilde{\alpha}_-^{-1}$ . To exclude bias, one has to consider the measurement of at least two kinematic points, resulting in  $\mu_1, \mu_2, \sigma_1, \sigma_2$ . Then, the expectation value of the mode  $b_{12}^{(2)}$  of  $p_1^{(2)} p_2^{(2)}$  is indeed unbiased,

$$E[b_{12}^{(2)}] = E\left[\frac{\mu_{\mathcal{C}_2}\sigma_{\mathcal{C}_1}^2 + \mu_{\mathcal{C}_1}\sigma_{\mathcal{C}_2}^2}{\tilde{\alpha}_- (\sigma_{\mathcal{C}_1}^2 + \sigma_{\mathcal{C}_2}^2)}\right] = \frac{1}{\tilde{\alpha}_-}. \quad (5)$$

To summarize, while both  $\mu_{\mathcal{C}_i}$  and  $\sigma_{\mathcal{C}_i}$  scale with  $b$ , the scaling of the Fierz variable  $\mathcal{F}_i = \mathcal{O}_i/b$  in Eq. (1) induces a  $b$ -dependent normalization factor which has to be removed. This also holds true for non-Gaussian distributions and, analogously, for more than one scaling factor. We have checked this result in numerical simulations for linear Fierz identities of the form  $E[\mathcal{O}_i/b] = 1$  and the two-observables, two-parameters case  $E[\mathcal{O}_{1,i}/b_1 + \mathcal{O}_{2,i}/b_2] = 1$ .

<sup>1</sup> Considering  $b$  instead of  $a$  avoids undefined expressions like  $E[1/\mu_{\mathcal{C}_j}]$  that arise if only one kinematic point  $j$  is considered. For the problem with more than one point, one can work with either  $a$  or  $b$ , as long as the pertinent pdfs are converted correctly at the end.

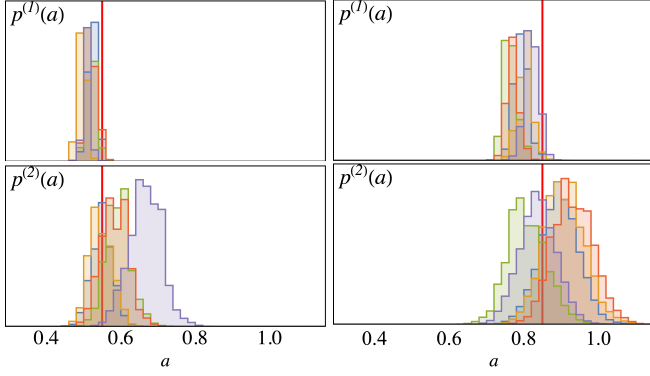


FIG. 1. Reconstruction of  $\tilde{\alpha}_-$  for Fierz identities with synthetic data. The figures show  $p^{(1)}(a) = \prod_i p(f_i^{(1)}) = \Delta f_i|a)$  and  $p^{(2)}(a) = \prod_i p(f_i^{(2)}) = 0|a)$  in the top and bottom row, respectively. Two choices of  $\tilde{\alpha}_-$  are shown (0.55, 0.85) with the thick red lines. Different colors of the histograms represent repetitions of the procedure to show fluctuations.

### 3. Non-linearity of the problem.

For the first Fierz identity given in Eq. (6) of the main text one has to consider squares of normal distributions. For a normally-distributed  $\mathcal{X} \sim \mathcal{N}[\mu, \sigma^2]$ ,  $\mathcal{Y} = \mathcal{X}^2$  is distributed according to a scaled, non-central  $\chi^2$  distribution with one degree of freedom (NC),

$$\begin{aligned} p_{\mathcal{Y}}(y) &= \int_{-\infty}^{\infty} dx \delta(x^2 - y) \frac{1}{\sqrt{2\pi}\sigma} \exp\left[-\frac{(x-\mu)^2}{2\sigma^2}\right] \\ &= \begin{cases} \frac{\exp\left[-\frac{y+\mu^2}{2\sigma^2}\right] \cosh\left[\frac{\sqrt{y}\mu}{\sigma^2}\right]}{\sqrt{2\pi y}\sigma} & \text{for } y > 0, \\ 0 & \text{else,} \end{cases} \quad (6) \end{aligned}$$

with mean and variance

$$\mu_{\mathcal{Y}} = \mu^2 + \sigma^2, \quad \sigma_{\mathcal{Y}}^2 = 2\sigma^2(2\mu^2 + \sigma^2), \quad (7)$$

demonstrating that, even if  $\tilde{\alpha}_-$  has the correct value  $\tilde{\alpha}_- = 1$ , the Fierz value  $\mathcal{F} = \mathcal{O}^2$  for the simple identity  $E[\mathcal{O}^2] = 1$  will no longer have an expectation value of one but  $E[\mathcal{F}] = \mu^2 + \sigma^2 = 1 + \sigma^2$ .

For the actual Fierz identity given in Eq. (6) of the main text, there is no closed-form expression for the difference of NC distributions and thus the distribution of the Fierz value  $\mathcal{F}_i^{(1)}$ , namely  $p^{(1)}(f_i^{(1)}|a, l, c)$  can only be obtained by sampling the set of observables  $\mathcal{O}_{j,i}$ , calculating  $f_i^{(1)}$  according to Eq. (6) of the main text for each sample, and then bin in  $\mathcal{F}_i^{(1)}$  for each kinematic point  $i$ .

To determine the distribution of  $a, l, c$  we note that expectation values add and then obtain from Eq. (7) that the expectation value of  $\mathcal{F}_i^{(1)}$  is given by

$$E[\mathcal{F}_i^{(1)}] = \sum_{j=1}^7 s_j \mu_{j,i}^2 + \sum_{j=1}^7 s_j \sigma_{j,i}^2 \quad (8)$$

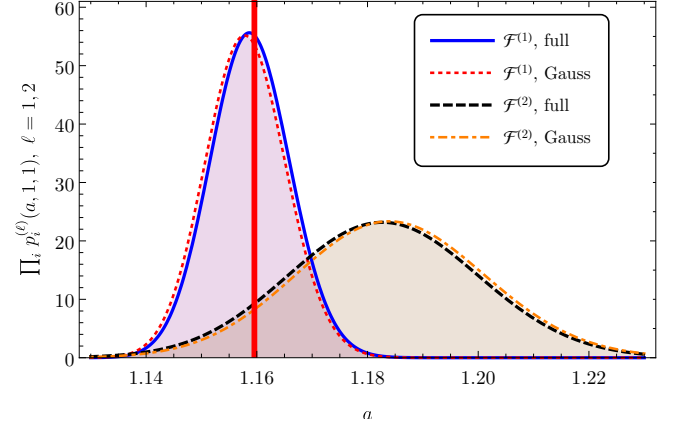


FIG. 2. Reconstruction of  $\tilde{\alpha}_-$  (vertical bar) from 500 sets of observables generated from the JüBo model. Shown are pdfs using the first and second Fierz identities. For both cases, full, nonlinear treatment according to Eqs. (10,13) and Gaussian approximations according to the two terms in Eq. (9) of the main text.

with  $\mathcal{O}_{j,i}$  and  $s_j$  specified in Table I. In Eq. (8), both sums are  $a, l, c$ -dependent.

On the other hand, we know that for the most probable  $a, l, c$  the expectation value has to be

$$\Delta f_i \equiv 1 + \sum_{j=1}^7 s_j \sigma_{j,i}^2 \quad (9)$$

to fulfill the Fierz identity, with  $\mathcal{O}_{j,i}$  and  $s_j$  specified in Table [tab:order]. The Fierz identity then imposes a condition on the distribution of Fierz values at each kinematic point  $i$ :

$$p_i^{(1)}(a, l, c) = p^{(1)}(f_i^{(1)} = \Delta f_i|a, l, c), \quad (10)$$

where again,  $\Delta f_i$  still depends on  $a, l, c$ . This is the first factor in Eq. (8) of the main text.

For the second Fierz identity given in Eq. (7) of the main text, the situation is similar. The distribution of the product of two independent Gaussian RVs,  $\mathcal{Z} = \mathcal{X}\mathcal{Y}$ , cannot be written in closed form but mean and variance can be calculated,

$$\mu_{\mathcal{Z}} = \mu_{\mathcal{X}}\mu_{\mathcal{Y}}, \quad \sigma_{\mathcal{Z}}^2 = \mu_{\mathcal{X}}^2\sigma_{\mathcal{Y}}^2 + \mu_{\mathcal{Y}}^2\sigma_{\mathcal{X}}^2 + \sigma_{\mathcal{X}}^2\sigma_{\mathcal{Y}}^2. \quad (11)$$

Compared to the squared case discussed before, there is no shift because  $E[\mathcal{X}\mathcal{Y}] = \mu_{\mathcal{Z}} = \mu_{\mathcal{X}}\mu_{\mathcal{Y}}$  and we simply have

$$E[\Sigma_i \mathcal{P}_i + ac(\mathcal{C}_{z,i}\mathcal{O}_{x,i} - \mathcal{C}_{x,i}\mathcal{O}_{z,i}) - \mathcal{T}_i] = 0, \quad (12)$$

because all Gaussian RVs enter either alone ( $\mathcal{T}$ ) or as products, but not as squares. Following the same arguments as for the first Fierz identity one obtains

$$p_i^{(2)}(a, l, c) = p^{(2)}(f_i^{(2)} = 0|a, l, c), \quad (13)$$

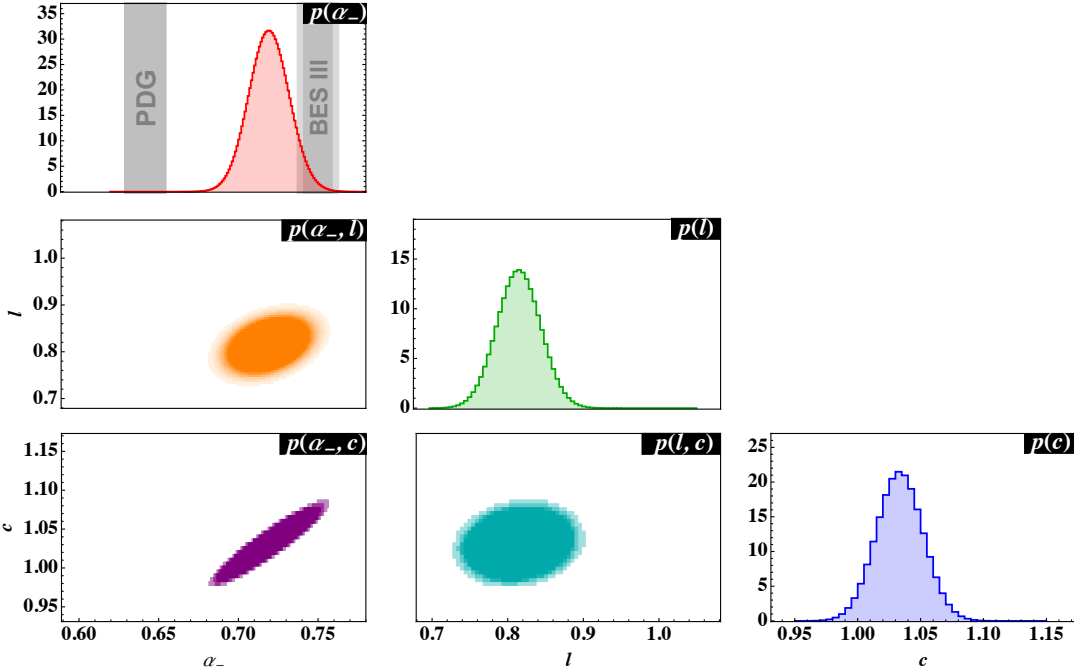


FIG. 3. Posterior distribution of  $(\alpha_-, l, c)$  as in Eq. (11) of the main text using a Gaussian prior with  $l \sim \mathcal{N}(1, 0.05^2)$ ,  $c \sim \mathcal{N}(1, 0.02^2)$ .

i.e., the second factor of Eq. (8) in the main text.

#### 4. Gaussian approximation.

For the first Fierz identity, we take account of the non-linearity of the problem because the r.h.s. of Eq. (10) is the distribution of the Fierz value, obtained through sampling and evaluated at  $f_i^{(1)} = \Delta f_i$  (analogously, for the second Fierz identity).

For the given data, the pdfs of the Fierz values are approximately Gaussian for both Fierz identities which suggests that a sufficiently accurate (partial) linearization of the problem might be possible. The Gaussian approximation of the first Fierz identity,  $p^{(1)}(f_i^{(1)}|a, l, c)$ , with variance  $\sigma_{\mathcal{F}_i^{(1)}}^2$ , evaluated at  $f_i^{(1)} = \Delta f_i$ , is

$$\begin{aligned} p_{G,i}^{(1)}(a, l, c) &\sim \exp \left[ -\frac{\left( \Delta f_i - \sum_j s_j (\mu_{j,i}^2 + \sigma_{j,i}^2) \right)^2}{2\sigma_{\mathcal{F}_i^{(1)}}^2} \right] \\ &= \exp \left[ -\frac{\left( 1 - \sum_j s_j \mu_{j,i}^2 \right)^2}{2\sigma_{\mathcal{F}_i^{(1)}}^2} \right], \end{aligned} \quad (14)$$

i.e., the numerator in the exponent is given by the difference  $\Delta f_i$  and  $E[\mathcal{F}_i^{(1)}]$  of Eqs. (9) and (8), respectively. The  $\sigma_{\mathcal{F}_i^{(1)}}$  are calculated from Eq. (7),

$$\sigma_{\mathcal{F}_i^{(1)}}^2 = \sum_{j=1}^7 2s_j^2 \sigma_{j,i}^2 (2\mu_{j,i}^2 + \sigma_{j,i}^2). \quad (15)$$

Notably, all variances in the numerator of the exponent cancel, irrespective of whether  $a, l, c$  are at their most probable value or not, and the resulting expression is very simple. This result corresponds to the first term of the exponent in Eq. (9) of the main text. An analogous approximation leads to the second term with  $\sigma_{\mathcal{F}_i^{(2)}}$  calculated from Eq. (11),

$$\begin{aligned} \sigma_{\mathcal{F}_i^{(2)}}^2 &= (al\sigma_{T_i})^2 + \sigma^2(l\mu_{\Sigma,i}, a\mu_{P,i}, l\sigma_{\Sigma,i}, a\sigma_{P,i}) \\ &\quad + \sigma^2(ac\mu_{C_z,i}, al\mu_{O_x,i}, ac\sigma_{C_z,i}, al\sigma_{O_x,i}) \\ &\quad + \sigma^2(ac\mu_{C_x,i}, al\mu_{O_z,i}, ac\sigma_{C_x,i}, al\sigma_{O_z,i}), \end{aligned} \quad (16)$$

where  $\sigma^2(\mu_1, \mu_2, \sigma_1, \sigma_2) \equiv \mu_1^2 \sigma_2^2 + \mu_2^2 \sigma_1^2 + \sigma_1^2 \sigma_2^2$  and  $\sigma_T$  is simply the uncertainty of  $T$ . Note that the  $a, l, c$  parameters still appear squared in the  $s_j$  terms of the first Fierz identity after the partial linearization of Eq. (14), see Table I. In general, such nonlinear problems are still biased. One can see this straightforwardly by following the arguments that led to Eq. (5): the proof for  $b$  being unbiased relies on the strict linear relation of parameter and data which is not given here anymore. Non-linear bias is usually neglected but should not be ignored. Therefore, we will test not only the full non-linear treatment but also the Gaussian approximation in the following through numerical simulations. As we will find, the bias is not large within uncertainties given our data base of around  $n = 300$  kinematic points.

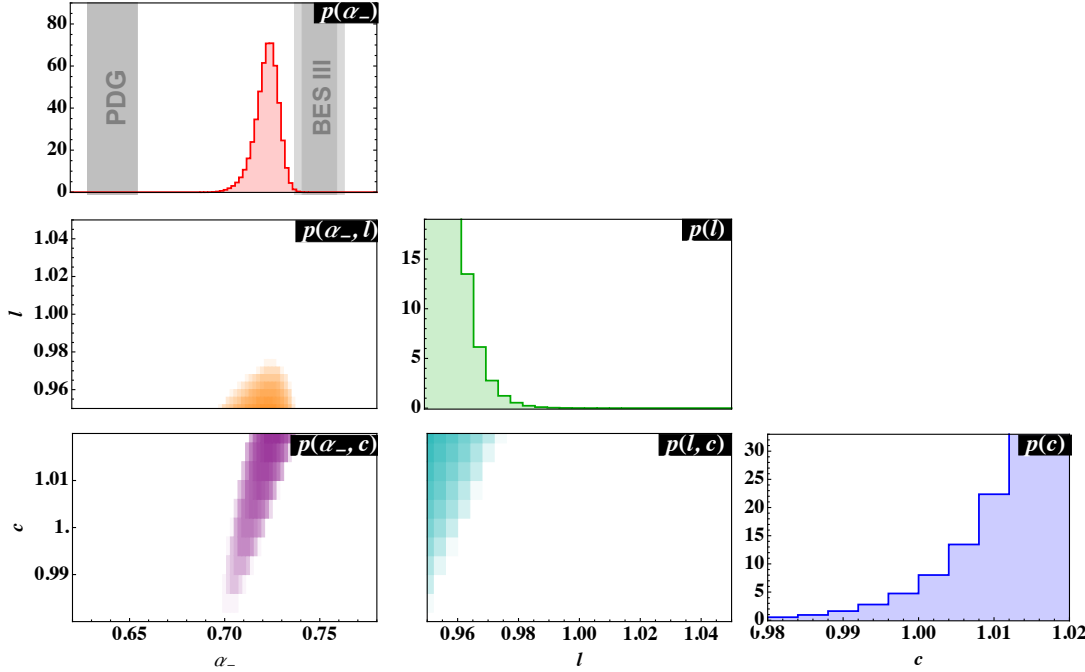


FIG. 4. Posterior distribution of  $(\alpha_-, l, c)$  as in Eq. (11) of the main text using a uniform prior with  $l \sim \mathcal{U}(0.95, 1.05)$ ,  $c \sim \mathcal{U}(0.98, 1.02)$ .

### Simulations with Synthetic Data

The method to extract  $\alpha_-$  relies on a numerical sampling procedure to construct the distributions of the Fierz values  $\mathcal{F}_i^{(1)}$  and  $\mathcal{F}_i^{(2)}$  that are subsequently evaluated at the respective expectation values  $f_i^{(1)} = \Delta f_i$  and  $f_i^{(2)} = 0$ . The remaining  $a, l, c$  dependence determines the distribution of these parameters. Also, for both calculations, the  $a, l, c$  dependence of normalization factors has to be removed as discussed previously. In the following tests, we fix  $l = c = 1$  for simplicity but we have also tested linear Fierz identities for two correction factors (see previous section).

First, we numerically test the method by generating synthetic data imposing different values of  $\tilde{\alpha}_-$  and then checking whether the distribution of the reconstructed  $a$  has its mode at  $a = \tilde{\alpha}_-$ . In Figs. 1 the result for both Fierz identities are shown. For each identity, values of seven observables  $j$  at 300 kinematic points  $i$  were generated that fulfill the respective Fierz identities. Gaussian noise was added using typical uncertainties of the observables, i.e.,  $\{\sigma_{C_{j,i}} | j = 1,..7\} = \{0.2, 0.25, 0.2, 0.15, 0.3, 0.25, 0.2\}$  and  $\{\sigma_{C_{j,i}} | j = 1,..7\} = \{0.1, 0.2, 0.2, 0.15, 0.1, 0.15, 0.2\}$  to first and second Fierz identity, respectively. Then, two different values of  $\tilde{\alpha}_- \neq 1$  were imposed to scale the respective observables  $C_{j,i}$  leading to  $\mathcal{O}_{j,i}$  from which  $\tilde{\alpha}_-$  was reconstructed. For each of the seven observables, 200,000 events were generated. The reconstruction process was then repeated a few

times, as the experimentally measured values  $\mu_{C_{j,i}}$  fluctuate. The results support the claim that the  $a = \tilde{\alpha}_-$  are indeed correctly reconstructed for both Fierz identities.

Second, the method was tested by using 500 sets of observables calculated from the JiBo model, where by construction the observables must obey the Fierz identities. These pseudodata were then rescaled by a value of  $\tilde{\alpha}_- = 1.157$  and Gaussian noise of realistic size was added to each observable. The test result is represented in Fig. 2. Again,  $\tilde{\alpha}_-$  is reconstructed within  $1-\sigma$  uncertainty. Here, we also test the Gaussian approximations from Eq. (9) of the main text together with the full, nonlinear treatment. For both identities, the differences are much smaller than the precision of  $a$ , based on the synthetic data that have similar uncertainties as the actual data.

This numerical test suggests that  $a$  is reconstructed from the second Fierz identity with about twice as large an uncertainty as that reconstructed from the first identity. This can be traced back to the essentially linear appearance of  $a$  in the second identity, compared to the quadratic appearance in the first identity.

This numerical test also provides the opportunity to assess the size of the different corrections applied in the extraction method of  $\alpha_-$ : If one evaluates  $f_i^{(1)}$  of the first Fierz identity at  $f_i^{(1)} = 1$  instead of  $f_i^{(1)} = \Delta f_i$ , the result is  $a = 1.136 \pm 0.007$ , i.e., too small by about  $3\sigma$ . Including the shift of the noncentral  $\chi^2$  distribution is therefore important (see item 3). If, in addition, one

does not remove the  $a$ -dependence of the normalization constant (see item 2), the result is  $a = 1.120 \pm 0.006$ , i.e., too small by more than five  $\sigma$ .

As demonstrated, the linearization of the problem in form of a Gaussian approximation provides very similar results to the full nonlinear treatment, at least for ideal data with only statistical noise. Another question is whether both methods are also *robust*. In an additional test, we have left the mean values  $\mu_{j,i}$  of the data unchanged but scaled all error bars  $\sigma_{j,i}$ , i.e., they no longer represent the statistical noise. With these modified data, the Gaussian approximations produce almost the same distributions of  $a$  while the results using the nonlinear method change noticeably. Therefore, all final results for the actual data shown in the supplemental material and main article are determined using the Gaussian approximations.

## DETAILED REPRESENTATION OF RESULTS

Using the procedure described above we can estimate the distribution of the Fierz values with respect to the asymmetry parameter  $\alpha_-$  and scaling factors  $l, c$  as well as their correlations. The latter two parameters represent an unknown systematic uncertainty on which priors have to be imposed as explained in the main text. We consider two extreme cases – Gaussian ( $l, c \sim \mathcal{N}(1, \delta_{l,c}^2)$ ) and Uniform priors  $l, c \sim \mathcal{U}(1 - \delta_{l,c}, 1 + \delta_{l,c})$  with  $\delta_l = 0.05$  and  $\delta_c = 0.02$ . The results are shown in Figs. 3 and 4.

## COMBINING MEASUREMENTS FROM TWO EXPERIMENTS

As mentioned in the main text, the measurements of the observables  $C_x$  and  $C_z$  were obtained from a separate experiment from the others ( $O_x, O_z, T, \Sigma, P$ ). We noted that whilst both experiments were carried out with the same CLAS detector, they took place during different run periods, and that this led to the data representing

a different set of kinematic bins in the variables  $W$  and  $\cos\theta$ . Fig. 5 shows the kinematic coverage of the two experiments. In order to interpolate the values and uncertainties of  $C_x$  and  $C_z$  to the points at which the other observables were measured, we used a Gaussian Process (GP) methodology.

In more detail, the uncertainties in the measured values of  $C_x$  and  $C_z$  are modelled by a first GP, optimizing the covariance function hyperparameters to give a best fit. This model of the uncertainties is then used to model the surfaces of  $C_x$  and  $C_z$  values in a second GP, where the result of the first GP is effectively used as a weighting. Covariance function hyperparameters are again optimized, and the resulting model can then be used to predict values and uncertainties of  $C_x$  and  $C_z$  at any point

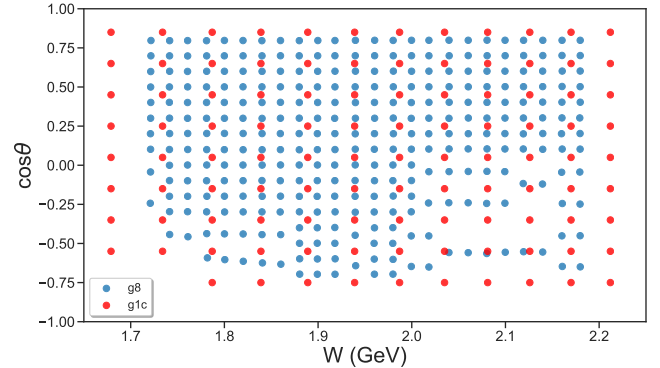


FIG. 5. Representation of the coverage of the two experiments used in this analysis. The red points are the values of  $W$  and  $\cos\theta$  at which the  $C_x$  and  $C_z$  observables were measured; the blue points are the values to which  $C_x$  and  $C_z$  are interpolated.

in the space of  $W$  and  $\cos\theta$ .

Figs. 6 and 7 illustrate the result of the interpolation for  $C_x$  and  $C_z$ . The interpolated values are plotted with the original values, where appropriate (see Fig. 5). The error bars represent  $2\sigma$ , in order to show more clearly that the GP method successfully models both the values and uncertainties of the observables.

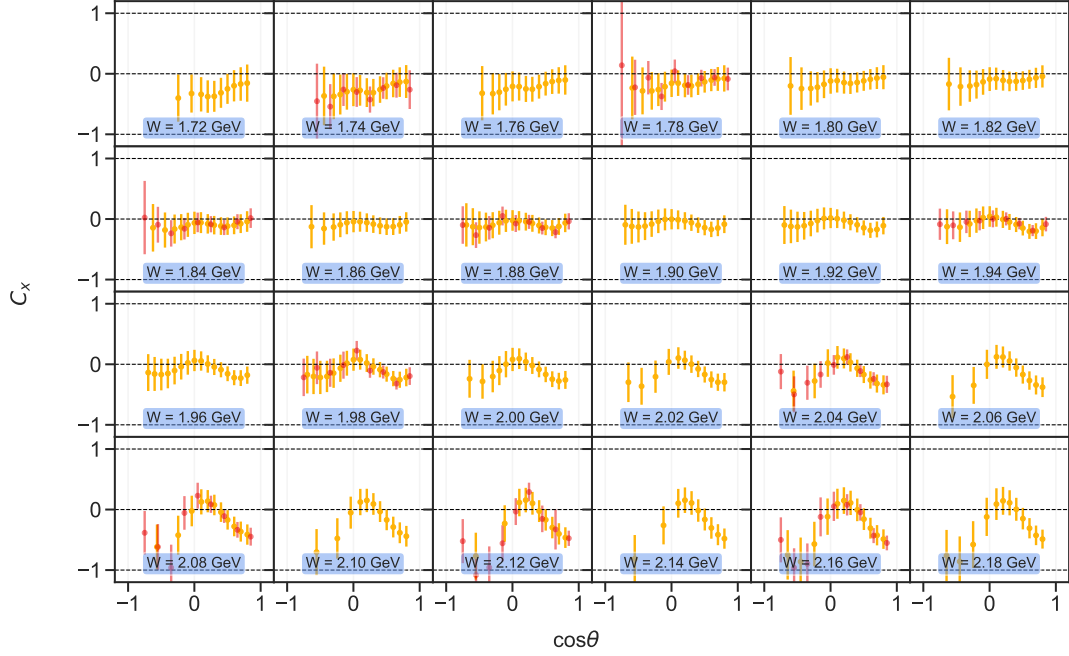


FIG. 6. Comparison of the original values of  $C_x$  (red points) and the interpolated values (amber points). The error bars as displayed represent  $2\sigma$ , to show the comparison more clearly.

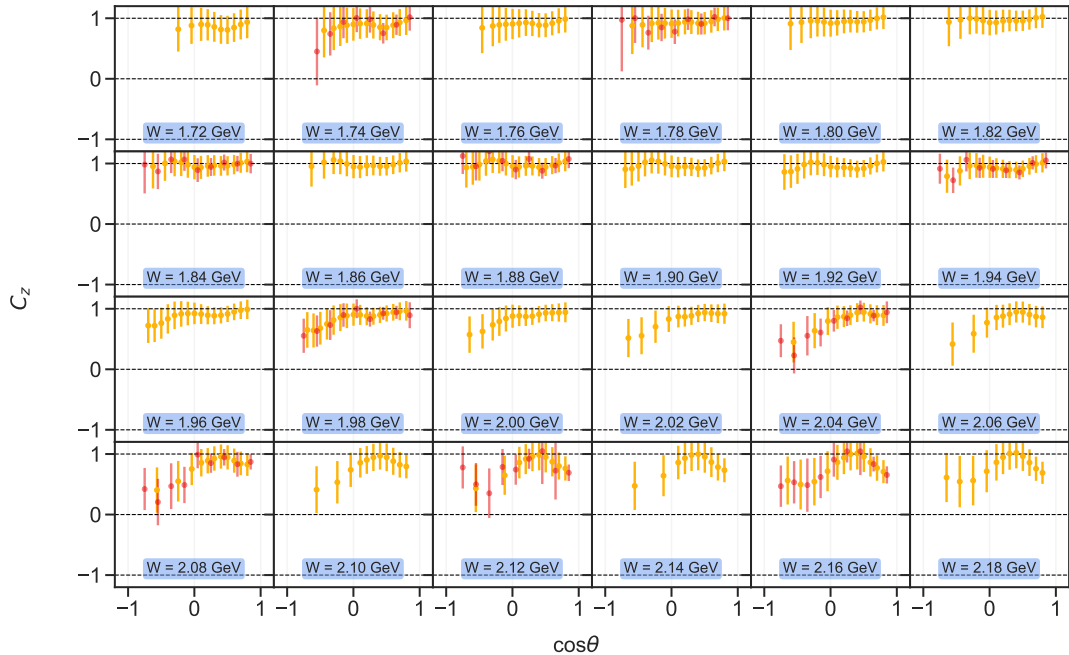


FIG. 7. Comparison of the original values of  $C_z$  (red points) and the interpolated values (amber points). The error bars as displayed represent  $2\sigma$ , to show the comparison more clearly.